3534 *Biochemistry* **2010,** *49,* 3534–3544
DOI: 10.1021/bi901957p

BIOCHEMISTRY
including biophysical chemistry & molecular biology
Article

In Vitro Recombination and Inverted Terminal Repeat Binding Activities of the *Mcmar1* Transposase[†]

Sylvaine Renault,*[,‡] Marie-Véronique Demattéi,[‡] Hichem Lahouassa, Yves Bigot, and Corinne Augé-Gouillou

Université François Rabelais de Tours, GICC, CNRS, UMR 6239, UFR des Sciences & Techniques, Parc de Grandmont, 37200 Tours, France. [‡]These authors contributed equally to this work.

Received November 13, 2009; Revised Manuscript Received March 26, 2010

ABSTRACT: The *Mcmar1 mariner* element (MLE) presents some intriguing features with two large, perfectly conserved, 355 bp inverted terminal repeats (ITRs) containing two 28 bp direct repeats (DRs). The presence of a complete ORF in *Mcmar1* makes it possible to explore the transposition of this unusual MLE. *Mcmar1* transposase (MCMAR1) was purified, and in vitro transposition assays showed that it is able to promote ITR-dependent DNA cleavages and recombination events, which correspond to plasmid fusions and transpositions with imprecise ends. Further analyses indicated that MCMAR1 is able to interact with the 355 bp ITR through two DRs: the EDR (external DR) is a high-affinity binding site for MCMAR1, whereas the IDR (internal DR) is a low-affinity binding site. The main complex detected within the EDR contained a transposase dimer and only one DNA molecule. We hypothesize that the inability of MCMAR1 to promote precise in vitro transposition events could be due to mutations in its ORF sequence or to the specific features of transposase binding to the ITR. Indeed, the ITR region spanning from EDR to IDR resembles a MITE and could be bent by specific host factors. This suggests that the assembly of the transposition complex is more complex than that of those involved in the mobility of the *Mos1* and *Himar1 mariner* elements.

Among transposable elements, *mariner*-like elements (MLEs)[1] and *Tc1*-like elements (TLEs) are DNA elements that move within eukaryotic genomes using a cut-and-paste transposition mechanism (*1*). MLEs and TLEs belong to the *IS630-Tc1-mariner* (*ITm*) superfamily and are widespread in eukaryotic genomes (*2*). The organization of *ITm* elements is very simple. They are composed of two inverted terminal repeats (ITRs) flanking a single open reading frame (ORF) that encodes a transposase (Tpase) with a DD[D/E] catalytic triad.

Over the past decade, there have been numerous studies of how TLE and MLE transposition works. They have shown that TLE and MLE ITRs are organized differently (*3*). The TLE ITRs vary in size (from 50 to 700 bp) and can contain one, two, or three Tpase binding sites that are conserved in sequence and correspond to direct repeats (DRs) within the ITR. One DR is always located at the outer end of the ITR, the others being located within the inner region of the ITR. The MLE ITRs are completely different. They are between 20 and 40 bp in size, and their sequence contains palindromic motifs (*4*). Another difference results from the fact that the MLE ITR is a complete binding site for the Tpase. This specificity avoids some of the terminological difficulties encountered with TLEs in defining and naming DRs, Tpase binding sites, and ITRs. In light of their ITR characteristics, and the origin of their Tpase DNA-binding domains, we recently extensively reviewed the literature in an attempt to clarify the assembly models for the transposition complex (also known as the "synaptic complex") of MLEs and TLEs. One conclusion was that transposition enhancers, corresponding to Tpase binding sites, occur in some TLE ITRs. We therefore concluded that the minimal synaptic complex results from the dimerization of TLE Tpases, bound to both the outer DRs, whatever the ITR size. The inner DR (found in TLEs with a long ITR) can be considered to be a transposition enhancer, because the binding of Tpase to these DRs sometimes increases the transposition efficiency by stabilizing the minimal synaptic complex (*3*). Factors such as HMGB1 have also been described as being a second kind of enhancer, affecting the transposition efficiency of some TLEs (*5*). ITR binding of MLE Tpases occurs only at the transposon ends, and no transposition enhancer has so far been identified for MLEs. However, it is suspected that *Mos1* UTRs may carry out this function, and internal sequences are indispensable for optimal transposition (*6*−*8*).

Mcmar1 belongs to the *elegans* subfamily of MLEs and is to date the only MLE described as having a long, 355 bp ITR, instead of the more common 20−40 bp MLE ITR (*9*). In contrast to most MLEs, *Mcmar1* ITRs are perfectly conserved in sequence and contain two DRs at their outer extremity that are separated

[†]This work was supported by grants from the CNRS, Ministère de l'Education Nationale, de la Recherche et de la Technologie, the Groupement de Recherche CNRS 2157, the European Commission (Project SyntheGeneDelivery, N°018716), and the University François Rabelais in Tours.

*To whom correspondence should be addressed: GICC, UMR CNRS 6239, Université François Rabelais, UFR des Sciences & Techniques, Parc de Grandmont, 37200 Tours, France. Telephone: +33 2 47 36 70 63, Fax: +33 2 47 36 70 42. E-mail: sylvaine.renault@univ-tours.fr.

[1]Abbreviations: BCC, bouillon coeur cerveau (heart brain broth); C, complex; CRO, cro binding domain; DR, direct repeat; DTT, dithiothreitol; EDTA, ethylenediaminetetraacetic acid; EMSA, electrophoresis mobility shift assay; HMGB, high-mobility group; IHF, interacting host factor; IPTG, isopropyl β-D-1-thiogalactopyranoside; ITm, IS TLE MLE family; ITR, inverted terminal repeat; MBP, maltose binding protein; MITE, miniature inverted terminal element; MLE, *mariner*-like element; neo, neomycin resistance gene; OD, optical density; ORF, open reading frame; TAE, Tris-acetate EDTA; Tet, tetracycline resistance gene; TLE, Tc1-like elements; Tpase, transposase; UTR, untranslated region.

 Published on Web 04/01/2010

by a 20 bp segment. *Mcmar1* ITRs therefore have convergent traits with some TLEs that have long ITRs, suggesting that they may contain transposition enhancers that function in a manner similar to that described for TLEs. *Mcmar1* contains an intact ORF encoding a Tpase of 350 amino acids (MCMAR1) that can be produced as a recombinant MCMAR1. In this paper, we focus on the recombination properties of MCMAR1 and on the assembly of ITR−Tpase complexes.

EXPERIMENTAL PROCEDURES

Oligonucleotides. The sequences of the oligonucleotides and primers used in this study are shown in Supporting Information 1. They were synthesized by Eurogentec.

Proteins. The gene encoding MCMAR1 was cloned in expression vector pMalc2x (New England Biolabs). For the cloning, the gene was amplified by PCR from a *Bam*HI DNA clone containing *Mcmar1-1* (*9*), using ORF1 and ORF2 as primers. The amplicon was cloned in pGEMT-easy (Promega) and then sequenced. The Tpase gene was then subcloned between the *Eco*RI and *Bam*HI sites in pMalc2x.

Escherichia coli (JM109) freshly transformed with pMal-Tpase and pRare (Novagen) was grown in 500 mL of BCC broth (beef heart and brain medium). The expression of MBP-Tpase was induced using 0.3 mM IPTG at an OD_{600} of 0.3 for 16 h at 25 °C. Cells were resuspended in 50 mL of 20 mM Tris (pH 9.0), 100 mM NaCl, and 0.1 mM DTT, frozen for 24 h, and finally lysed with 0.5 mg/mL lysozyme for 30 min at 4 °C. The cell debris was centrifuged, and 50 mL of the supernatant was used to purify MBP-Tpase on 1 mL of amylose resin (New England Biolabs), according to the manufacturer's instructions. The resulting protein (MBP-MCMAR1) will be designated "MCMAR1".

The purified IHF and the purified HMGB, DSP1, of *Drosophila melanogaster* were kind gifts from R. Chalmers (University of Oxford, Oxford, United Kingdom) and D. Locker (University of Orléans, Orléans, France), respectively.

Cloning of the 355 bp ITR and the Deleted ITR. The 355 bp Δ300−355, Δ262−355, Δ200−355, Δ142−355, and Δ79−355 ITRs were obtained by PCR amplification from a *Bam*HI DNA clone containing *Mcmar1-1* (*9*). The PCRs were conducted using the 355KX1 primer to anneal at the 5′ outer end of the 355 bp ITR, and the primers annealing in the 3′ inner ITR region to amplify the 355 bp ITR (355KX2), the Δ300−355 ITR (300KX), the Δ262−355 ITR (262KX), the Δ200−355 ITR (200KX), the Δ142−355 ITR (142KX), and the Δ79−355 ITR (79KX). The Δ1−80 and Δ1−160 ITR fragments were also amplified by PCR using the primer 355KX2 to anneal at the 3′ inner end of the 355 bp ITR, and primers 80 and 160, respectively. The PCR products were cloned in pGEMT-easy, and their sequences were checked.

The EDR and IDR were obtained by annealing two complementary oligonucleotides: EDR1 and EDR2 for the EDR and IDR1 and IDR2 for the IDR. These two oligonucleotides are designed for construction of flush extremities that are compatible with *Kpn*I at the 5′ extremity, and with *Xho*I at the 3′ extremity. Once annealed, the oligonucleotides were phosphorylated and cloned in pBC KS+ (Stratagene) within the *Kpn*I and *Xho*I sites.

Transposition Assays. To make the *Mcmar1* transposon donor plasmid, pBC-355Tet355, the *Hin*dIII−*Xba*I fragment, containing the promoterless gene encoding the tetracycline resistance of plasmid pBC3Tet3 (*10*), was first cloned in the pBCKS+ vector digested by *Hin*dIII and *Xba*I (pBC-Tet). The *Mcmar1* full-length ITR and variants were amplified with two sets of primers, *Kpn*I-ITR (355KX1) with XbaI-ITR (355KX2, 300KX, 262KX, 200KX, 142KX, and 79KS), and NotI-ITR (355NS1) with SacI-ITR (355NS2, 300NS, 262NS, 200NS, 142NS, and 79NS) for the 355 bp Δ300−355, Δ262−355, Δ200−355, Δ142−355, and Δ79−355 ITRs, respectively. The sequences of the primers are listed in Supporting Information 1. They were cloned in pGEMT-easy and finally checked by sequencing. The *Kpn*I−*Xho*I and *Not*I−*Sac*I fragments were then cloned into pBC-Tet to make the final version of pBC-355Tet355. To obtain the pSW-355pTet355 plasmid, the promoterless Tet gene was replaced with the Tet gene and its promoter (pTet) in pBC-355Tet355. The *Hin*dIII and *Xba*I pTet fragments were obtained from pSW-3′pTet3′ (*11*). The *Kpn*I−*Sac*I fragment containing 355-pTet-355 was cloned at the corresponding sites in pSW29 (*12*).

In vitro transposition and in vitro excision assays were performed in 5% glycerol, 10 mM Tris (pH 9.0), 50 mM NaCl, 50 mM EDTA or 20 mM $MgCl_2$, 5−100 nM MCMAR1, and 600 ng of pBC-355Tet355 or pBC-Tet in a 20 μL reaction mixture at 30 °C for 3 h; 300 ng was analyzed by electrophoresis on a 0.8% agarose gel with TAE1X buffer. *E. coli* DH5α was electroporated with 60 ng of transposition assay and then plated on 12.5 μg/mL tetracycline LB medium. For interplasmid transposition, 300 ng of pSW-355pTet355 and 300 ng of pBC were used under the same reaction conditions as for pBC-355Tet355, and 60 ng of target plasmid was electroporated.

For in vivo transposition assays, the JM109 strain of *E. coli* was cotransformed with the vector expressing MCMAR1, pKK-Tnp, and the pseudotransposon pBC-355Tet355. We created a negative control by cotransforming an empty pKK233-2 vector with pBC-355Tet355. Fifteen clones were taken and individually grown in 2.5 mL of LB. After 1 h at 37 °C, the production of Tpase was induced via addition of 0.3 mM IPTG. Cells were grown for 5 h at 32 °C, and the number of cells was counted on LB and LB with tetracycline. The transposition rate was estimated by dividing the number of tetracycline-resistant (TetR) cells by the number of cells in the culture.

DNA Sequencing. Sequencing of DNA plasmids and fragments was performed by MWG Biotech. The primers used for sequencing were Tet1 and Tet2, the universal and reversal M13 primers being those supplied by MWG-biotech (Supporting Information 1).

Electrophoretic Mobility Shift Assays (*EMSAs*). ^{32}P-labeled probes were prepared by cleaving the ends of the different ITRs cloned in pGEMT or pBC, with *Eco*RI for the 355 bp Δ300−355, Δ262−355, Δ200−355, Δ142−355, and Δ79−355 ITRs and the *Kpn*I−*Xho*I fragment for the EDR and IDRs. ^{32}P-labeled probes of the mutant EDR, deleted EDR, and IDR were obtained by annealing 100 pmol of complementary oligonucleotides (sequences in Supporting Information 1) with an extension of two T residues at the 3′ end. We made the labeled probes by filling the ends with [α-^{32}P]dATP and Klenow DNA polymerase. The fragments were purified on a 6% acrylamide/bisacrylamide gel eluted in 100 mM Tris (pH 7.5) and 200 mM NaCl, overnight at room temperature, precipitated, and resuspended in water.

Δ79−355 EDR and IDR 200 bp in length were obtained by amplification with primers pU and pRev (Supporting Information 1) situated on either side of the MCS of the pGEMT and pBC plasmids.

Binding was performed in 5% glycerol, 10 mM Tris (pH 9.0), 50 mM NaCl, 5 mM EDTA or 20 mM $MgCl_2$, 90 nM MBP-MCMAR1, and 5 fmol of ITR in 20 μL of the reaction mixture, at 4 °C for 15 min or at 30 °C for 2 h. Complexes were separated

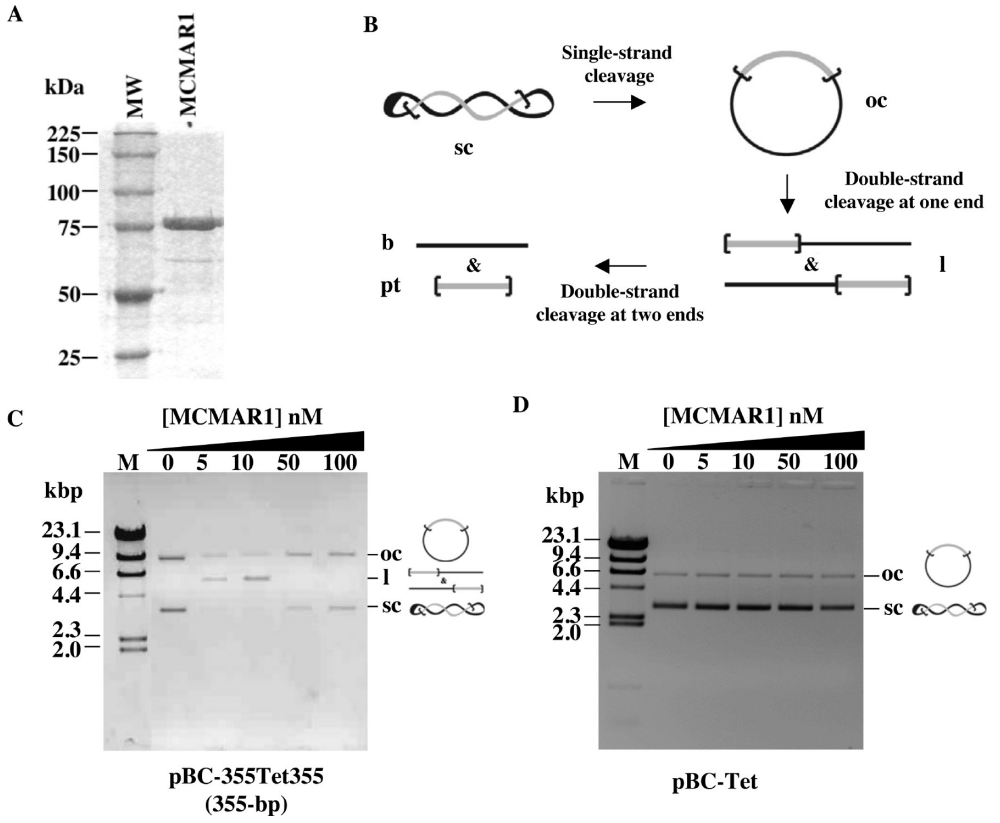

FIGURE 1: Excision activity of MCMAR1. (A) MCMAR1 purification. MW is molecular weight. (B) Excision assay principles. In the presence of transposase, the first strand cleavage of a supercoiled plasmid (sc) containing a pseudotransposon leads to the formation of an open circle (oc). After the second strand cleavage at one ITR end, the plasmid will be linear (l). At the end of the process, the double-strand cleavage at the two ITR ends leads to the appearance of the backbone (b) and the pseudotransposon (pt). (C) pBC-355Tet355 (300 ng) was cleaved for 3 h at 30 °C with MCMAR1 concentrations ranging from 0 to 100 nM, as indicated. Lane M contained molecular weight markers (400 ng of λDNA cleaved with *Hin*dIII). oc denotes the open circle plasmid, l the linear plasmid, and sc the supercoiled plasmid. (D) Similar assays were performed using pBC-Tet.

on 6% acrylamide/bisacrylamide gels (30:0.93) in 0.25× TBE [22 mM Tris (pH 8.0), 22 mM boric acid, and 0.6 mM EDTA] at 200 V for 2 h and then autoradiographed. In assays to confirm the binding specificity, 1 μg of pBSsk+DNA (Stratagene) or sheared herring sperm DNA was used as a nonspecific competitor, and 1 μg of pGEMT-ITR, pBC-EDR, or pBC-IDR was used as a specific competitor.

Footprint. Binding of Tpase with ITR was performed in 5 mM EDTA as described above. The complexes were cut off the gel and processed directly in the gel by the Cu/phenanthroline method. The gel slides were equilibrated in 10 mM Tris (pH 8.0) for 5 min. Complexes were treated with 200 μL of 2 mM 1,10-phenanthroline and 0.46 mM $CuSO_4$ and for various times after the addition of 200 μL of 58 mM 3-mercaptopropionic acid. The reaction was stopped by the addition of 200 μL of 28 mM 2,9-dimethyl-1,10-phenanthroline. DNA was eluted from the gel in 10 mM Tris (pH 7.5), 0.1 mM EDTA, and 200 mM NaCl overnight at room temperature. DNA was precipitated and resuspended in 80% formamide, 10 mM NaOH, 1 mM EDTA, 0.1% xylene cyanol, and bromophenol blue and denatured before being separated on a 6% sequencing gel in 1× TBE. The ITR probes were sequenced by the Maxam and Gilbert method.

RESULTS

MCMAR1 was produced in bacteria as a C-terminal fusion with the maltose binding protein (MBP) and purified to 98% by affinity chromatography (Figure 1A). The ability of MCMAR1 to promote single-strand, double-strand DNA cleavages and a complete transposon excision was first assayed in vitro using pBC-355Tet355 as a pseudo-*Mcmar1* donor plasmid with different amounts of Tpase. The plasmid pBC-355Tet355 consists of the two full-length 355 bp ITRs flanking the promoterless, tetracycline-resistant gene. If DNA cleavages were to occur under our experimental conditions, we would expect that accumulation of an open circle plasmid will result from single-strand cleavages, that of a linear plasmid from a double-strand DNA cleavage at one transposon end, and that of excised products from two double-strand cleavages at both transposon ends (Figure 1B). Reduced amounts of the superhelical and open circle plasmid and an accumulation of the linearized plasmid were observed when the reactions were performed with 5−10 nM MCMAR1 (Figure 1C). This revealed that single- and then double-strand DNA cleavages had occurred at one transposon end. No cleavage was observed at 0, 50, or 100 nM Tpase. Whatever Tpase concentration was used, assays monitored with a plasmid that did not contain the *Mcmar1* ITR (Figure 1D) displayed no DNA cleavage, confirming that MCMAR1 had not been contaminated by traces of nuclease. We concluded that the cleavage probably occurred at the end of the *Mcmar1* ITR. Complete excisions were never observed, since neither the pBC backbone nor the excision product (the pseudotransposon) was detected on the agarose gel, whatever the Tpase concentration, incubation time (up to 16 h), or temperature (25, 30, or 37 °C) (data not shown).

Despite the fact that cleavage analyses did not reveal any transposon excision, in vitro transposition assays were performed to determine whether MCMAR1 was able to achieve strand transfers leading to plasmid recombination or transposition events. Assays were performed with Tpase concentrations ranging from

5 to 100 nM and with pBC-355Tet355 as the transposon donor and the target plasmid, as described previously (*11*). Briefly, the pseudotransposon containing the tetracycline resistance (Tet^R) gene without its promoter is excised by the transposase from the donor plasmid and integrated in a new locus. The Tet^R gene is expressed only when the pseudotransposon is integrated under the control of a promoter. In this assay, tetracycline-resistant clones result from transposition. After bacterial transformation and selection on tetracycline, resistant clones were recovered only at low Tpase concentrations (5 and 10 nM), in agreement with the results of cleavage. Under identical experimental conditions, when pBC-355Tet355 is replaced with pBC-Tet (which lacks both ITRs), no tetracycline-resistant clones were recovered. This indicated that obtaining tetracycline-resistant clones with pBC-355Tet355 was dependent on the Tpase concentration and on the presence of the *Mcmar1* ITR. DNA plasmids from 34 tetracycline-resistant clones were purified and analyzed by digestion and sequencing (Supporting Information 2). The results revealed two kinds of plasmid with a complex structure, corresponding to two (26 clones) or three (eight clones) plasmids fused by recombination. They were recovered after cleavages and strand transfer exchanges that very probably occurred at the outer ends of the *Mcmar1* ITR (Supporting Information 2). Interestingly, and in agreement with the results obtained in cleavage assays, we found that only one transposon end was involved for the cleavage and strand transfer reactions that led to all these plasmid fusion products. In an attempt to determine whether it was possible to detect transposition events from excised elements, we then used a two-plasmid assay. The first, a "suicide" pSW-355pTet355 plasmid (which contained an R6K replication origin and carried the tetracycline resistance gene with its promoter), was the donor for pseudotransposon 355-pTet-355, and the second pBC plasmid, which does not contain the ITR, was the target for integration. The pseudotransposon is excised by the transposase from the suicide donor plasmid and integrated into the target plasmid. Only heteroplasmid recombination events, including transposition or co-integration, can be detected using this transposition assay, because the suicide donor plasmid cannot replicate in the DH5α strain of *E. coli*. After in vitro transposition, bacterial transformation, and selection, no Tet^R clones were obtained in the control experiments monitored with the suicide plasmid containing no ITR. In contrast, numerous Tet^R clones were obtained in assays monitored with the suicide donor plasmid and pBC plasmids. The plasmids contained in 11 independent Tet^R clones were purified and analyzed on an agarose gel after enzymatic digests and then sequenced, using primers anchored in the Tet^R gene. Only one kind of plasmid was obtained (Supporting Information 3). This plasmid corresponded to integration of a fragment from the donor suicide plasmid into the target plasmid and resulted from a DNA strand exchange that occurred at a site located between 10 and ~300 bp from the outside of one ITR (Supporting Information 3).

Taken together, these data demonstrate that (1) the optimum concentration of the MCMAR1 protein ranges from 5 to 10 nM, as previously found for HIMAR1 (*13*); (2) in vitro transposition assays do not allow recovery of cardinal transposition events; and (3) the fusion events do not occur exactly at the outer end of the ITR, indicating that the DNA cleavages and strand transfers are not as precise as with MOS1 or HIMAR1 (*14*−*16*).

The modalities of DNA binding of MCMAR1 to its ITR might be responsible for the imprecise DNA cleavages and strand transfers observed in vitro. This was therefore further investigated by electrophoretic mobility shift assays (EMSAs) using the 355 bp ITR as the probe under various conditions of Tpase concentration, temperature, and cations (Figure 2A). Complexes are detected under all conditions when using 100 nM MCMAR1 (Figure 2A, lanes 6−9), whereas complexes are more difficult to observe when using 10 nM MCMAR1 (Figure 2A, lanes 2−5). However, the detection of cleavage products at 30 °C in the presence of $MgCl_2$ supported the possibility that ITR−MCMAR1 complexes existed at both concentrations (Figure 2A, lanes 5 and 9). For the study, the best condition for the observation of complexes was retained, i.e., 100 nM MCMAR1. The specificity of ITR binding was verified under the best conditions for assembly of complexes (Figure 2B). Three shifted bands and Tpase−ITR aggregates were detected (lane 2). The main complex was C2, whereas C1 and C3 were detected only as thin bands. As previously demonstrated for other MLE ITRs (*10*, *13*, *17*, *18*), MBP was unable to bind the 355 bp ITR (data not shown), indicating that MCMAR1 is able to bind stably to its ITR. MCMAR1 binding specificity was verified in an EMSA, using pBS as a nonspecific DNA competitor (lane 3), and confirmed using pBS-ITR355 as a specific competitor, which eliminated the shifted bands (lane 4). In addition, MCMAR1 did not bind the *Mos1* ITR (data not shown), highlighting the fact that MCMAR1 binds specifically to its own ITR.

We then searched for MCMAR1 binding sites throughout the whole ITR. The 355 bp ITR exhibited different sequence features: two large palindromes of ~60 and ~100 bp, seven direct repeats of 8−9 bp, and two 28 bp direct repeats (DRs), both presenting similarities in sequence to the ITR of *Cemar1* (*9*). Nine ITR variants were used in the EMSA, with MCMAR1: seven variants containing the DR (EDR, IDR, Δ79−355, Δ142−355, Δ200−355, Δ262−355, and Δ300−355) and two variants that did not contain the EDR or IDR (Δ1−80 and Δ1−160) (Figure 2C). The ability of MCMAR1 to bind to each of the nine fragments was investigated in EDTA at 30 °C. All the ITR variants, except Δ1−80 and Δ1−160, allowed complexes to assemble, similar to what is observed with the 355 bp ITR (Figure 2D). In addition, C2 was always the most abundant complex, and ITR−MCMAR1 aggregates were detected in several wells. However, IDR is not very efficient in forming Tpase complexes, as demonstrated by the overexposure required to detect the shifted bands.

The EMSA results therefore indicated that the first 79 bp of the ITR contained two binding sites for MCMAR1, the EDR and IDR. Due to the fact that ITR Δ1−80 lacks the ability to form any complex with the Tpase, the EDR and IDR are the only binding sites for MCMAR1 within the 355 bp full-length ITR. The EDR is a strong binding site, and the IDR is a weak binding site. This is in agreement with published data showing that (in the *Mcmar1* ITR) only the EDR and IDR have sequences similar to that of the *Cemar1* ITR, the binding site for *Cemar1* Tpase (*9*). Furthermore, the EMSA patterns were similar, whichever probe was used. An EMSA with the Δ79−355 variant or with the EDR was also performed under conditions for transposition (10 nM) and for visualization of complexes (100 nM) (Figure 3A,B). The same results were obtained with the two different transposase concentrations even if the complexes were more easily detected with 100 nM MCMAR1, as previously observed with the 355 bp ITR (Figure 2A). All further experiments were conducted with 100 nM MCMAR1.

The binding specificity of both DRs was verified in an EMSA using a nonspecific or specific competitor (data not shown). Taken together, these data indicated that the *Mcmar1* Tpase

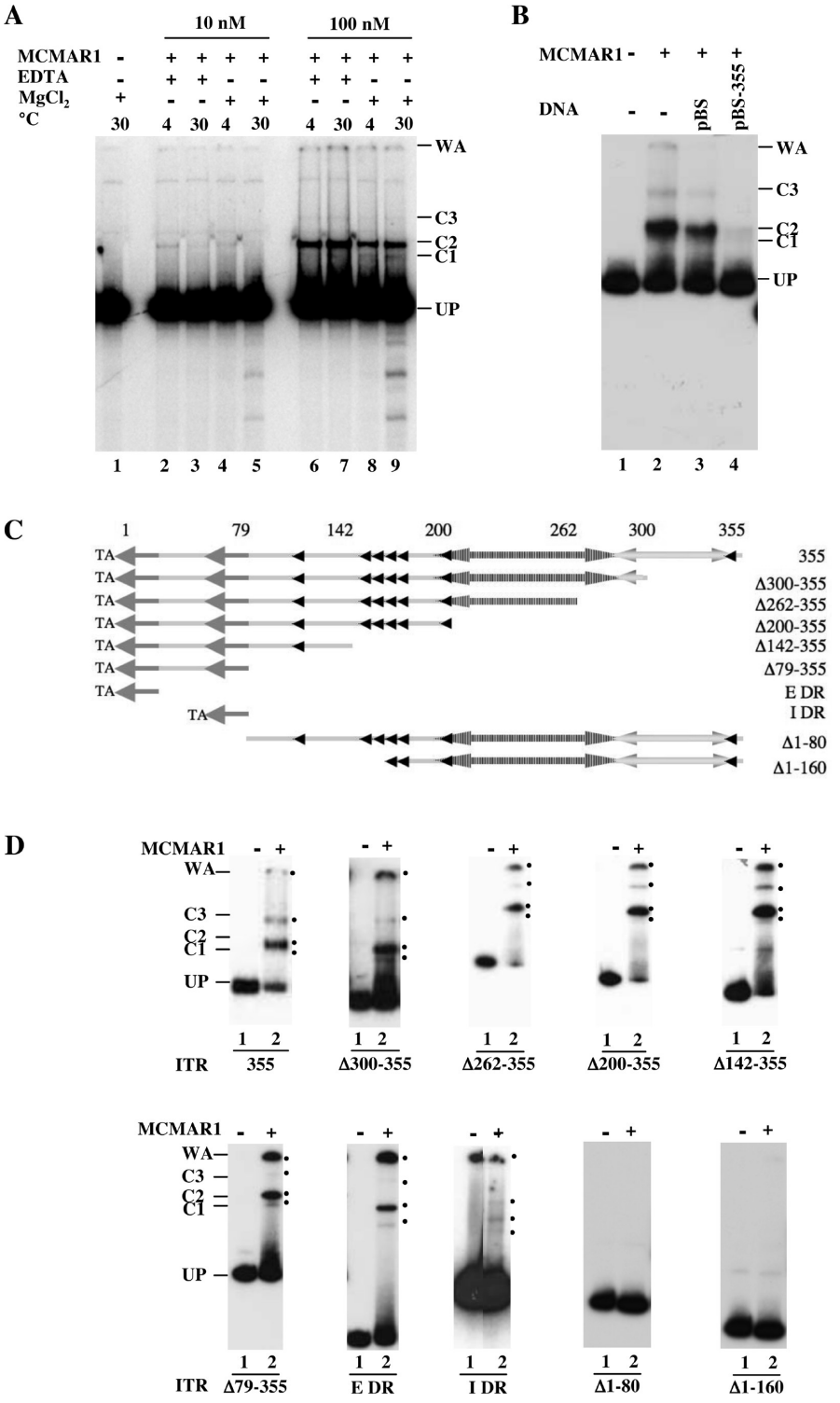

FIGURE 2: ITR binding of MCMAR1. (A) MCMAR1−355 bp ITR complexes obtained under different conditions of assembly, 4 °C (lanes 2, 4, 6, and 8) or 30 °C (lanes 1, 3, 5, 7, and 9), in the presence (+) or absence (−) of 5 mM EDTA (lanes 2, 3, 6, and 7) or 20 mM $MgCl_2$ (lanes 4, 5, 8, and 9). Complexes were assembled at 30 °C for 2 h and at 4 °C for 30 min with 10 nM (lanes 2−5) and 100 nM MCMAR1 (lanes 6−9), respectively. UP denotes the unbound probe. C1−C3 denote MCMAR1−ITR complexes, and WA denotes MCMAR1−ITR aggregates. (B) Specificity of MCMAR1 binding. MCMAR1−355 bp ITR complexes were obtained with 100 nM Tpase in 5 mM EDTA, without competitors (lane 2), with a non-specific competitor (lane 3), or with a specific competitor (lane 4). (C) Schematic representation of the full-length and 3′-truncated versions of 355 bp ITR. Nine ITR variants were designed: seven 3′-truncated ITRs (Δ300−355, Δ262−355, Δ200−355, Δ142−355, Δ79−355, Δ1−80, and Δ1−160) and the external (EDR) and internal (IDR) direct repeats (gray arrows within the 80 first nucleotides). Black-tipped arrows correspond to short direct repeats of 9 bp. The two double arrows (positions 200−280 and 281−355) represent two distinct palindromic regions. (D) Location of MCMAR1 binding sites using nine deleted ITR variants. UP denotes the unbound probe. C1−C3 denote MCMAR1−ITR complexes, and WA denotes MCMAR1−ITR aggregates. EMSA analysis of MCMAR1 binding to different ITRs, with (+; lane 2) or without (−; lane 1) MCMAR1.

might interact with two sequences within the 355 bp ITR, EDR, and IDR, albeit less efficiently with the IDR sequence. To confirm this point, we performed competition reactions in an EMSA using a radiolabeled Δ79−355 ITR and equimolar amounts of cold Δ79−355 ITR, EDR, or IDR (Figure 4A). In contrast to the Δ79−355 ITR and EDR, the IDR was unable to switch off the

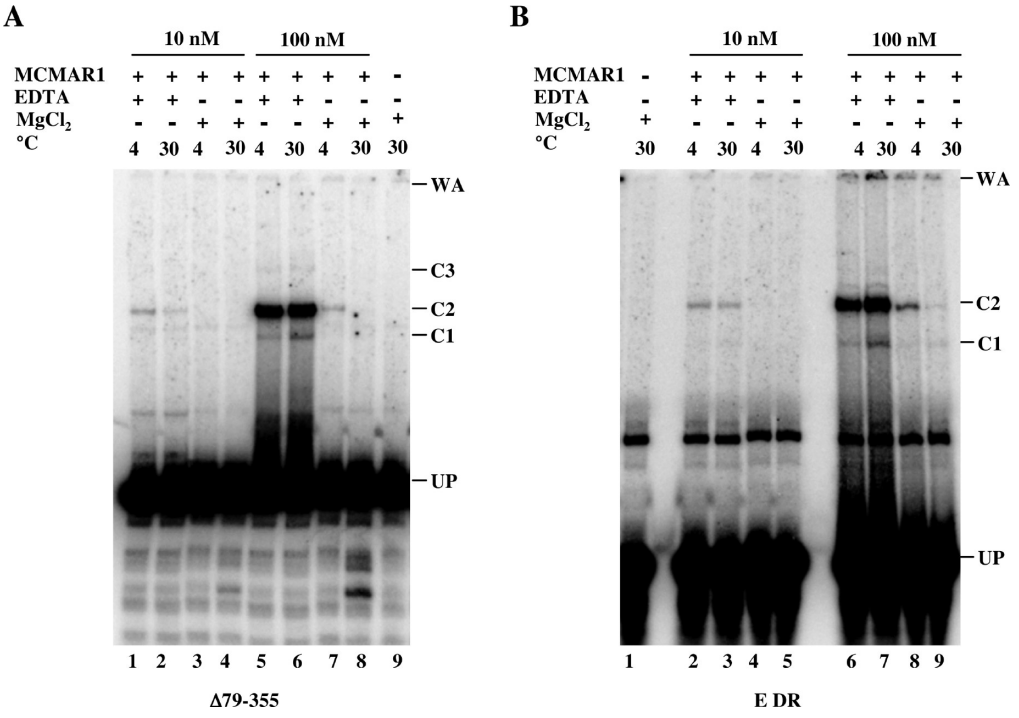

FIGURE 3: EMSA of Δ79−35 and EDR with MCMAR at 10 and 100 nM. Complexes were assembled under differents conditions with 50 mM EDTA (lanes 1, 2, 5, and 6 for Δ79−355 and lanes 2, 3, 6, and 7 for the EDR) or 20 mM $MgCl_2$ (lanes 3, 4, and 7−9 for Δ79−355 and lanes 1, 4, 5, 8, and 9 for the EDR) and at different temperatures (4 °C for lanes 1, 3, 5, and 7 for Δ79−355 and lanes 2, 4, 6, and 8 for the EDR or 30 °C for lanes 2, 4, 6, 8, and 9 for Δ79−355 and lanes 1, 3, 5, 7, and 9 for the EDR) with two different concentrations of transposase MCMAR1 (10 nM for lanes 1−4 for Δ79−355 and lanes 5−8 for the EDR and 100 nM for lanes 2−4 for Δ79−355 and lanes 1, 3, 5, 7, and 9 for the EDR) . The complexes consisted of two deleted ITRs, Δ79−355 and EDR.

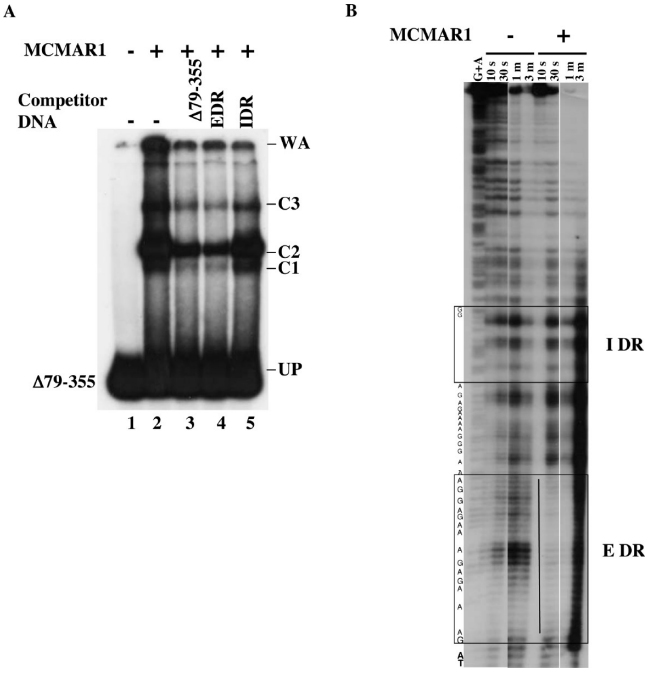

FIGURE 4: EDR is the preferential binding site for MCMAR1. MCMAR1 binding to the Δ79−355 bp ITR. EMSAs were conducted without a DNA competitor (lane 2) or with a 5-fold excess of the unlabeled Δ79−355 ITR (lane 3), EDR (lane 4), or IDR (lane 5). UP denotes the unbound probe. C1−C4 denote MCMAR1−ITR complexes, and WA denotes MCMAR1−ITR aggregates. (B) Footprinting analysis. Various Cu-phenanthroline treatment times were applied to the end-labeled, 355 bp ITR in the presence (+) or absence (−) of MCMAR1. A Maxam−Gilbert sequencing (G+A) was performed on the same labeled 355 bp ITR to scale the Cu-phenanthroline footprints.

Tpase−ITR complexes. Further analysis has shown that the competition effect is the only one detected; indeed, EMSA patterns were not modified via addition of a short cold probe (EDR) to the Δ79−355 ITR sample. This strongly suggested that C1−C3 contained only one DNA fragment. The preference of MCMAR1 for binding to the EDR was also verified using chemical footprints, with the 355 bp ITR as the probe (Figure 4B). They revealed one main protected area of ~28 bp that spanned the EDR, whereas the protection of the IDR was not detected. This confirmed that MCMAR1 preferentially bound to the EDR.

The composition of ITR−MCMAR1 complexes was then analyzed. Our intention was first to examine the stoichiometry of MCMAR1 in complexes (C1−C3) formed with the EDR. The simplest hypothesis proposes that C1−C3 contain one, two, and three molecules of MCMAR1, respectively. This point was investigated in cross-linking experiments with EDR or Δ79−355 and MCMAR1, using various different cross-linking agents: glutaraldehyde, formaldehyde, UV irradiation, *cis*-platinum, and *cis*-hydroxyplatinum as described previously (*15*, *19*). The addition of glutaraldehyde, formaldehyde, and *cis*-platinum completely destabilized the assembled complexes, which prevents the detection of cross-linking (data not shown). UV irradiation and addition of *cis*-hydroxyplatinum did not reveal any cross-linking between MCMAR1 and these ITRs, probably because the reactive sites of the transposase and the ITR are too far from each other to be cross-linked with UV or *cis*-hydroxyplatinum (data not shown). According to the hypothesis just mentioned, the fact that C2 is the most abundant complex suggests that MCMAR1 is mainly bound as a dimer on a single EDR, as previously shown for HIMAR1 (*13*) and MOS1 (*15*). We therefore performed a set of experiments to map the organization of

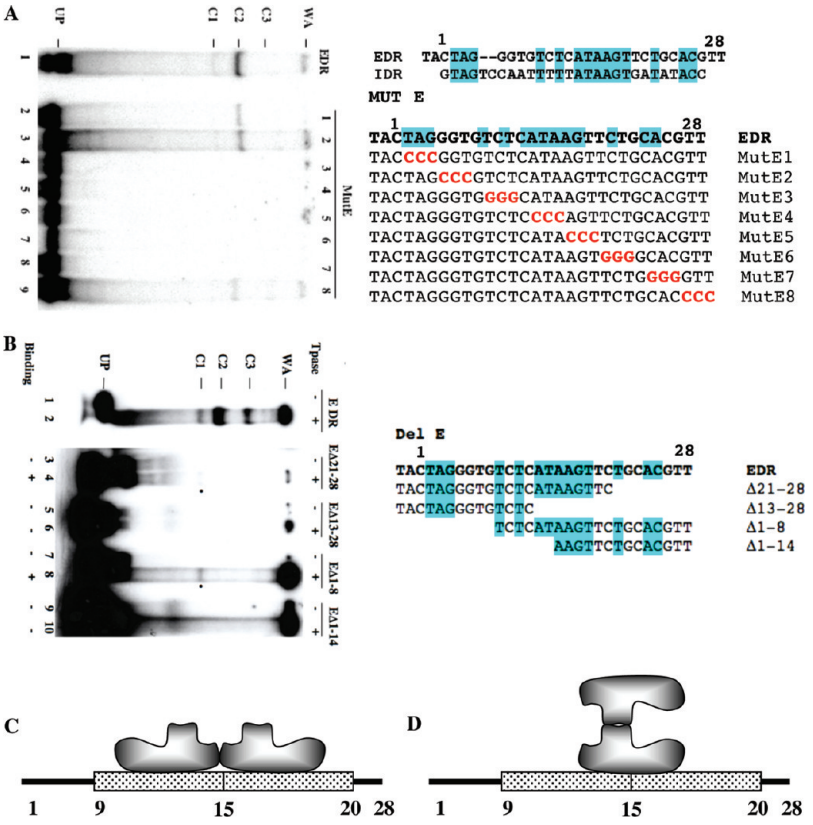

FIGURE 5: MCMAR1 binding within the EDR. (A) On the right, sequences corresponding to mutated EDR are given (MutE1−E8). Mutated positions are colored red. On the left, the corresponding EMSA analyses are presented. (B) On the right, the sequences corresponding to 5′- and 3′-truncated versions of EDR (EΔ21−28, EΔ13−28, EΔ1−8, and EΔ1−14) are given. Conserved positions between DR are highlighted in blue. On the left, the corresponding EMSA analyses are presented. The presence or absence of shifted bands is indicated under each lane. The duration of the autoradiography for the EDR was 2 h (−80 °C), whereas 4 days (−80 °C) was required for the deleted probes. (C and D) Schematic representations of the binding of a dimer of MCMAR1 to the EDR in *cis* (C) or in *trans* (D).

the MCMAR1 binding site within the EDR. Alignment of the sequences for the EDR and IDR revealed a well-conserved 14 bp motif (Figure 5A). The fact that MCMAR1 is less efficiently bound to the IDR than to the EDR suggests that these conserved positions are involved, probably in MCMAR1 binding, but are not sufficient to stabilize the binding. To dissect the MCMAR1 binding site(s), and to identify which nucleotides within the DR are most important for binding as well as for stabilizing MCMAR1, an EMSA was employed to assess the interactions between the Tpase and several EDR mutants. Analyses were focused on the EDR, the high-affinity binding site.

First, mutants of the EDR were used to determine which part of the EDR is indispensable for binding MCMAR1. EMSAs were performed using mutant EDRs at different positions as probes (Figure 5A). Complexes were only detected with EDR mutants 1, 2, and 8 (Figure 5A). These results showed two things. First, bases 7−25 of the EDR all constitute the binding site of MCMAR1, and second, the main complex still observed is the C2 complex, confirming that MCMAR1 was mainly bound as a dimer to the EDR.

A complementary approach was designed to detect and identify the MCMAR1 monomer binding site within the EDR. We therefore hypothesized that whether MCMAR1 binds mainly as a dimer to the EDR (positions 7−25), each monomer forming the dimer might be in contact with the DNA, thus defining two half-binding sites. We used truncated EDRs as probes in EMSAs. Two deleted EDRs, EΔ1−8 and EΔ21−28, were bound very weakly by MCMAR1 as C1 complexes (one ITR per Tpase), whereas the other two deleted DRs were no longer bound (Figure 5B). These findings showed that when the 7 bp at the 3′ end is deleted (Δ21−28), the dimer is no longer able to bind to the EDR. Only a weak signal (C1 complex) was observed, suggesting that a binding site for a monomer was still present between positions 1 and 20. The same analysis was conducted with the deletion in the 5′ part of the EDR; the C1 complex was observed with EΔ1−8 but not EΔ1−14, showing that a binding site for a monomer was probably present between positions 9 and 20.

These results could be interpreted in two ways; either two half-sites are occupied by a dimer (Figure 5C), or only one central site (positions 9−20) is the binding site of two *in-trans* associated monomers (Figure 5D). According to both hypotheses, our data provided evidence that the EDR is a binding site for a Tpase dimer between bases 9 and 20. It can be noted that this region of both DRs is well-conserved between the EDR and IDR, suggesting that a dimer of MCMAR1 is bound to this region in both DRs.

Classical short/long probe analyses in EMSA were developed to define the number of ITRs in complexes involving the EDR and Δ79−355 ITR. Short (40 and 85 bp), labeled probes for the EDR and Δ79−355 ITR, respectively, and long (200 and 260 bp) cold fragments for the EDR and Δ79−355 ITR, respectively, were used (Figure 6). Whichever probe was used, all three complexes (C1−C3) were observed in the absence of the long fragments. When equimolar amounts of the long cold fragment were added (lanes 3), no additional complex was detected, as would be expected if at least one complex contains two ITRs (as in paired-end complexes). Similar results were obtained when the

amounts of the long cold fragment were increased 2−10-fold (not shown). These findings confirmed the data presented in Figure 3A.

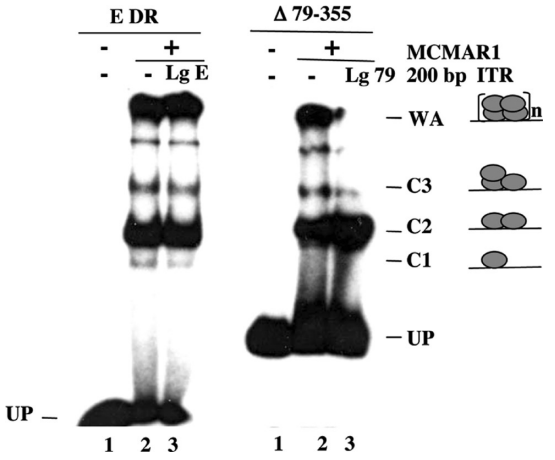

FIGURE 6: PEC detection. Complexes were assembled without (−; lane 2) or with (+; lane 3) a cold 200 bp derivative of the E or Δ79−355 ITR (here termed LgE and Lg79, respectively), together with the labeled E and Δ79−355 ITR, and were separated by an EMSA. The molecular composition of each complex is shown on the right. UP denotes unbound probe. C1−C3 denote MCMAR1−ITR complexes, and WA denotes MCMAR1−ITR aggregates.

Taken together, our results indicate that the complexes involving the EDR and Δ79−355 ITR are not paired-end complexes, but single-end complexes. We therefore wondered whether these minimal binding sequences would allow transposition to occur. Interplasmid transposition assays similar to those previously described with the pSW-355pTet355 plasmid were monitored, using a pSW-[Δ79−355ITR]pTet[Δ79−355ITR] (2.8 kb) or pSW-EDRpTetEDR (2.7 kb) plasmid as a "suicide" transposon donor, and pBC (3.4 kbp) as the integration target. In contrast to assays conducted with the pSW-355pTet355 plasmid, very few Tet^R clones were obtained with these donors. Analysis of 15 of them (3 and 12, respectively) revealed that no cardinal transposition event occurred (Figure 7A). Nevertheless, two kinds of plasmid were obtained. The first corresponded to fusion of pSW-355pTet355 and pBC plasmids (6.1 kb) and resulted from DNA strand exchanges that occurred at a site located between 10 and 300 bp from the outside of one ITR (Figure 7B; zero and three clones, respectively). The second type corresponded to plasmids (from 4.7 to 5 kb) containing imprecise transposition events, in which either 1 and 100 bp ITRs (one and seven clones, respectively) or 10−300 bp ITRs (two clones each) from the flanking regions of the donor plasmids were found at one or both transposon ends (Figure 7C).

Since these minimal ITR variants were not sufficient to promote precise transposition, we hypothesized that host factors

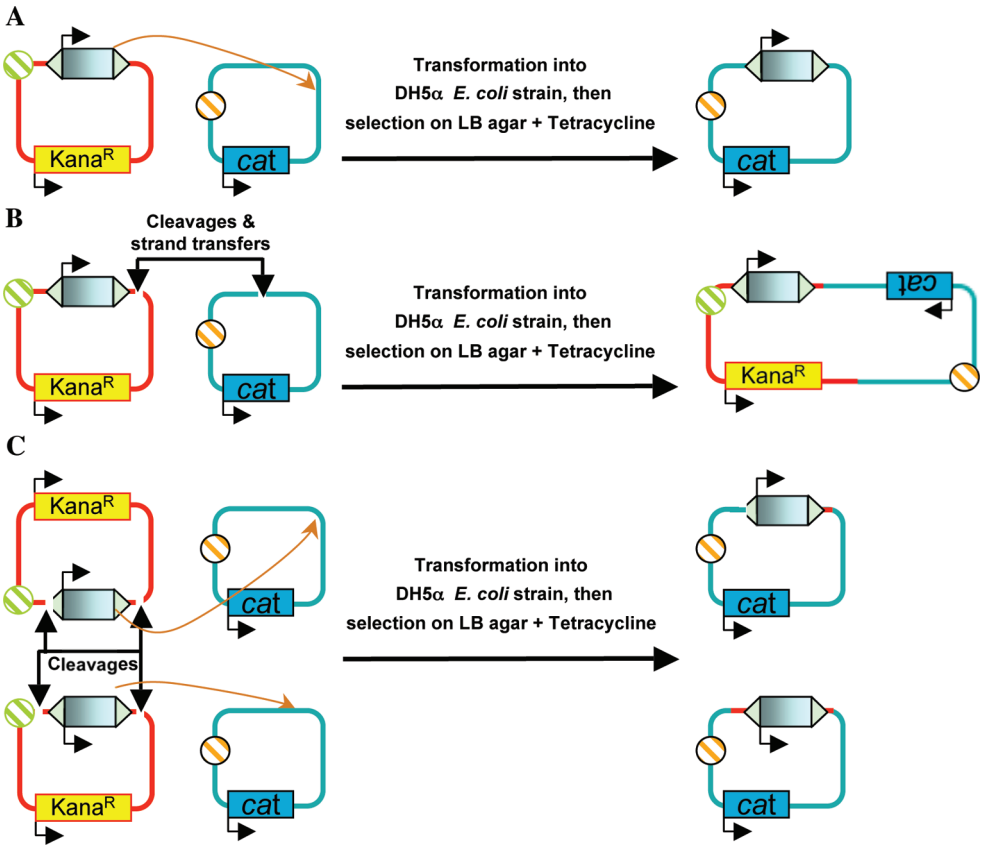

FIGURE 7: Transposition products resulting from assays performed with two plasmids, pSW-[Δ79−355ITR]pTet[Δ79−355ITR] and pSW-EDR-pTet-EDR as the transposon donor and pBC as the integration target. (A) Schematic representation of the expected in vitro transposition. In the transposon donor plasmids, pSW-[Δ79−355ITR]pTet[Δ79−355ITR] or pSW-EDR-pTet-EDR, the Δ79−355ITR and EDR ITR (arrows), tetracycline gene (light blue boxes) with its promoter (the arrow at one end locates its promoter), and the origin of the R6K replication (hatched circle with green lanes) are represented. The gene encoding the resistance to tetracycline is shadowed in black around the start codon. In the pBC plasmid used as the integration target, the *cat* (chloramphenicol acetyltransferase) gene (turquoise box with an arrow at one end that locates its promoter) and the origin of ColE1 replication (hatched circle with orange lanes) are represented. (B) Schematic representations of the events that lead to the formation of plasmid fusion. (C) Schematic representations of the events that lead to integrations of imprecisely excised transposons. Backbones are represented by red−blue and turquoise lanes in the donor and target plasmids, respectively.

could be necessary for complete transposition to occur. Some factors are known to bend DNA, thus promoting the assembly of DNA−protein complexes. They consist of specific proteins such as IHF and the HMG proteins. IHF displays some interaction sequence specificity, and a consensus sequence has been reported [WATCAANNNNTTR (*20*)]. This consensus is present in the IDR of the *Mcmar1* ITR. In contrast, HMGB proteins interact with DNA, in a manner independent of sequence. The HMGB−DNA interaction specificity is conferred by accessory proteins (*21*). Interestingly, these proteins have already been associated with the transposition of some DNA transposable elements, Tn*10* and *Sleeping Beauty* (*5*, *22*). First, we investigated the possible involvement of the α/β IHF heterodimer of *E. coli* (*22*) and the HMGB region of DSP1, a gene of *D. melanogaster* (*23*), in assembly of the *Mcmar1* complex, using the 355 bp, Δ79−355 ITR, and EDR; 355 bp ITR−IHF complexes were detected by an EMSA under conditions of IHF specific binding (Figure 8A). Similar results were obtained with DSP1 (Figure 8B). Despite the fact that the consensus IHF binding site is located within the IDR, no complex was detected between the IDR or EDR and IHF (data not shown). In contrast, the α/β IHF heterodimer bound to the Δ79−355 ITR to form two distinct complexes (Figure 8A), suggesting that there is an IHF binding site between the two DRs. Interestingly, the probe was totally shifted, suggesting that IHF binding occurs with high affinity. Similar data were obtained when DSP1 was used as the bending protein (Figure 8B). Our data therefore demonstrate that both the HMGB domain and IHF were able to interact with the 355 bp and Δ355 ITRs in addition to MCMAR1. In both cases, their binding sites were located between the EDR and the IDR.

To test the role of these two host factors in transposition, in vivo transposition assays were performed in *E. coli* for IHF and in HeLa cells for HMGB.

As the IHF protein is naturally produced in *E. coli*, in vivo *E. coli* transposition assays were performed with the pBC-355Tet355 plasmid as the donor and target plasmid (*10*). Approximately 13 Tet^R clones were analyzed, and none of them displayed the pattern expected for transposition (data not shown). In fact, all Tet^R clones were due to Tpase-dependent plasmid fusions.

The HMGB1 protein is present in every human cell. A plasmid containing a pseudotransposon was constructed via insertion of the neomycin-resistant gene (Neo^r) between two 355 bp ITRs. The pseudotransposon donor plasmid and a plasmid expressing MCMAR1 were cotransfected in HeLa cells. The rate of transfection was controlled by cotransfecting a plasmid expressing the luciferase gene. Cells resistant to neomycin were selected for 14 days with G418. The number of Neo^r cells was counted and compared to the number of cells cotransfected with a plasmid containing Neo^r but without the ITR or MCMAR1. There was no statistical difference between the rates of Neo^r clone formation obtained with or without MCMAR1. This finding suggests that MCMAR1 is very probably inactive in mammal cells or that HeLa cells do not contain the host factors required to perform *Mcmar1* transposition.

DISCUSSION

The *Mcmar1-1* element is unusual among MLEs. This element has two large, perfectly homologous, 355 bp ITRs instead of the more common 28−30 bp ITR. The length and structure of the ITR (which includes two DRs) are more similar to those of the TLE. *Mcmar1-1* is also one of the few MLEs so far known to possess a full-length ORF. This combination of a large ITR and a Tpase ORF allowed us to investigate the functioning of this unusual element at the interface of the TLE and MLE, even though the phylogenetic analysis unambiguously showed that MCMAR1 is an MLE transposase (*24*).

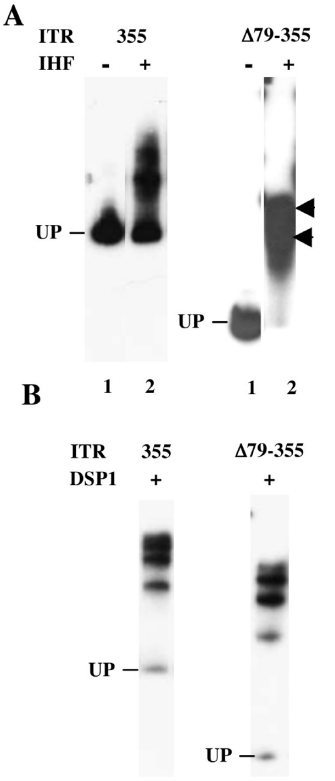

FIGURE 8: Binding of IHF and DSP1 to the 355 bp and Δ79−355 ITR. Complexes were assembled for 2 h at 30 °C, in the presence (+) or absence (−) of (A) IHF (10 nM) and (B) DSP1 (100 nM) with the 355 bp and Δ79−355 ITR. The concentrations used for IHF and DSP1 are those described for specific binding (*22*, *23*). UP denotes unbound probes.

Our results show that MCMAR1 is able to bind to its ITR, to perform single- and double-strand DNA cleavage, and to accomplish strand transfers. It is also able to mediate the transfer of fragments from one plasmid to another and to achieve full transposition of imprecisely excised elements. It is noticeable that these recombination events were all ITR- and Tpase-dependent. In contrast, our results showed that MCMAR1 is unable to trigger in vitro cardinal transposition. As far as we are aware, this is the first time that a result of this type has been reported for a eukaryotic transposon, except for the Tpases and transposon derived from *Bythogrea thermydron* and *Alvinella caudata* MLE (*25*). Currently, two types of Tpases are differentiated on the basis of their transposition mechanisms. Examples of the first type include MOS1, the "resurrected" HIMAR1, MBOUMAR, the Tpase encoded by exon 3 of SETMAR, and *Sleeping Beauty*, which all perform all transposition steps (*26*−*29*). The second type cannot produce any transposition or recombination event; examples of this type include the *Musca domestica* and *Blatella germanica* MLEs (*30*) and the *Pacmar1* MLE (*31*).

Two nonexclusive properties of MCMAR1 may be responsible for its limited ability to produce cardinal transposition in vitro. First, the MCMAR1 sequence displays some slight differences from those of other MLE Tpases. For example, a FQQDGR-APH motif is present instead of FLHDNAPH, and a TVPHDL

motif is present instead of the highly conserved WVPHEL motif. The FQQDGRAPH motif includes the second D of the catalytic triad and looks like that found in active TLE Tpases. We have made MCMAR1 mutants in which the FQQDGRAPH sequence is replaced by the FLHDNAPH sequence, and the TVPHDL sequence by the WVPHEL sequence, which contain both changes. Our results showed that these three MCMAR1 mutants are no more able to mediate transposition than the wild-type MCMAR1 (personal data). MCMAR1 may also have accumulated one or more inactivating mutations since its introduction into the genome of *Meloidogyne chitwoodi*. One possible way to circumvent this problem would be to reconstruct the active copy from sequences available in databases, which has already been done for *Sleeping Beauty*, *Frog Prince*, and *Himar1* (*27*, *29*, *32*). Molecular reconstruction requires large sequence collections, and to date, only two *Mcmar1* copies are available, *Mcmar1-1* and *Mcmar1-2*, the second being an internally deleted version of *Mcmar1-1* (*9*). The recent genome sequencing of two related *Meloidogyne* species, *Meloidogyne hapla* and *Meloidogyne incognita*, has not yielded any new copies related to *Mcmar1* (*33*, *34*). This lack of data therefore makes it impossible to use this strategy to verify the activity of MCMAR1.

In spite of these problems with the MCMAR1 sequence, we must point out that this protein has kept all its Tpase activities, its only defect being that it performs imprecise DNA cleavages and strand transfers. Our results also reveal that the interaction of MCMAR1 with its ITR could also be dependent on host factors, such as HMG-like proteins. As highlighted by our results, this property could be due to more complex modes of ITR binding and synaptic complex assembly than those proposed for other MLEs (*3*, *35*, *36*). Different mutually exclusive hypotheses may account for complex(es) formed with MCMAR1. The first one considers that the EDR is in fact the usual 30 bp ITR found in other MLEs and that the binding of MCMAR1 to the IDR is negligible in the complex assembly. From this point of view, the homology detected between the EDR and IDR is random, due to the short length of both DRs. In this case, as for other MLEs, a dimer is bound to the EDR and the synaptic complex is not correctly formed due to mutations in the transposase. The second hypothesis considers that the *Mcmar1* ITR contains two DRs and looks like the structure observed in the TLE ITR. The binding of MCMAR1 to the subterminal repeat (IDR) would help the formation of a productive synaptic complex as for *Sleeping Beauty*, the organization of the DR being in *cis* or in *trans* (Figure 9A) (*37*, *38*). The third hypothesis comes from the sequence analyses, which indicate that the outer region of the 355 bp *Mcmar1* ITR could originate from an 80 bp MITE. Indeed, the EDR and IDR have been well-conserved as inverted repeats and are separated by a 20 bp palindromic linker (Figure 9B). This configuration is generally considered to be typical of a MITE (*39*) and is very close to that of the 80 bp MITE named *miHsmar*, originating from the *Hsmar1* MLE (*18*, *40*). The assembly of MCMAR1 on the pseudo-MITE ITR could lead to the elaboration of a complex involving two or four transposases (Figure 9C). One may wonder whether this special organization is involved in the peculiar features observed in DNA cleavages and strand transfers. We also found that the 79 bp outer nucleotides of the ITR are enough to allow fragment transfers between plasmids, and the transposition of imprecisely excised elements to occur at a lower frequency than the complete ITR; we therefore supposed that the 275 bp in the inner region of the ITR could act as an enhancer, as previously reported for the *Tc3* ITR and *Mos1*

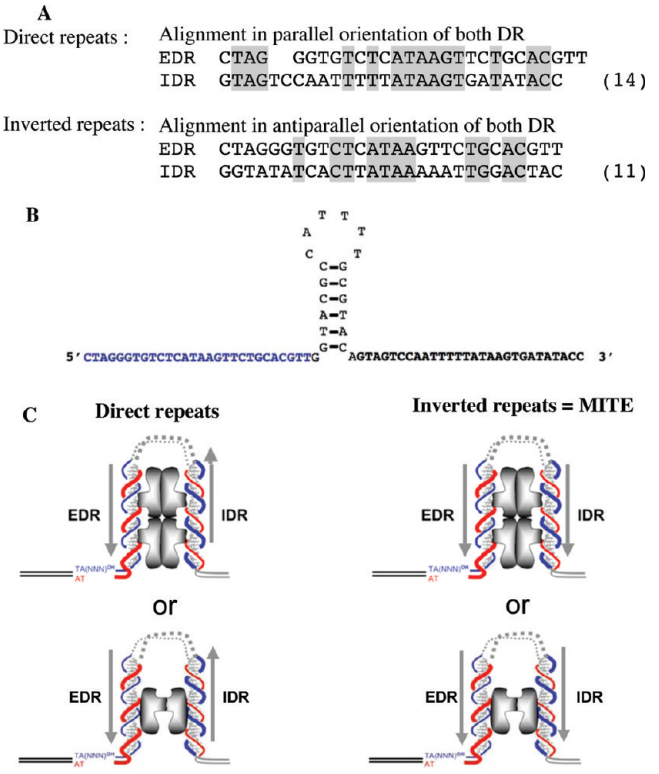

FIGURE 9: Schematic representation of intra-ITR pseudosynaptic complex assembly involving the EDR, the IDR, and MCMAR1. (A) Sequence alignments of both DRs in parallel or antiparallel. Conserved positions are highlighted in gray, and their occurrences are numbered in parentheses. (B) Diagrammatic representation of the palindrome of the 20 bp spacer located between the EDR (bold blue letters) and IDR (bold black letters). (C) Schematic representation of the intra-ITR, pseudosynaptic complex with the EDR and IDR considered as a direct repeat (left) or an inverted repeat (right).

UTR (*3*, *8*). Overall, these observations suggest that *Mcmar1* may be a chimeric MLE, which has replaced its original ITR with a closely related MITE at both ends and then co-evolved until it reached the current version of *Mcmar1* with a large and complex ITR.

ACKNOWLEDGMENT

We thank Dr. Benjamin Brillet and Dr. Nicolas Buisine for their expert help regarding *mariner* Tpase biochemistry and protein cross-linking and for fruitful discussions. We also thank Dr. Pierre Abad (INRA Antibes) for the gift of the *Mcmar1-1* clone and Dr. Ronald Chalmers (University of Oxford) and Prof. Daniel Locker (University of Orléans) for kindly supplying bacterial IHF, DSPI, and rat HMGB1 protein samples, respectively. We thank the two anonymous reviewers for their helpful comments. The English text has been revised by Dr. M. Ghosh.

SUPPORTING INFORMATION AVAILABLE

Oligonucleotide sequences used and structure of the plasmids obtained after a transposition assay with three different plasmids. This material is available free of charge via the Internet at http://pubs.acs.org.

REFERENCES

1. Wicker, T., Sabot, F., Hua-Van, A., Bennetzen, J. L., Capy, P., Chalhoub, B., Flavell, A., Leroy, P., Morgante, M., Panaud, O., Paux, E., SanMiguel, P., and Schulman, A. H. (2007) A unified classification system for eukaryotic transposable elements. *Nat. Rev. Genet. 8*, 973–982.

2. Shao, H., and Tu, Z. (2001) Expanding the diversity of the *IS630-Tc1-mariner* superfamily: Discovery of a unique DD37E transposon and reclassification of the DD37D and DD39D transposons. *Genetics 159*, 1103–1115.
3. Brillet, B., Bigot, Y., and Augé-Gouillou, C. (2007) Assembly of the *Tc1* and *mariner* transposition initiation complexes depends on the origin of their transposase DNA binding domains. *Genetica 130*, 105–120.
4. Bigot, Y., Brillet, B., and Augé-Gouillou, C. (2005) Conservation of palindromic and mirror motifs within the inverted terminal repeats of *mariner-like* elements. *J. Mol. Biol. 351*, 108–116.
5. Zayed, H., Izsvak, Z., Khare, D., Heinemann, U., and Ivics, Z. (2003) The DNA-bending protein HMGB1 is a cellular cofactor of *Sleeping Beauty* transposition. *Nucleic Acids Res. 31*, 2313–2322.
6. Tosi, L. R., and Beverley, S. M. (2000) *Cis* and *trans* factors affecting *Mos1 mariner* evolution and transposition *in vitro*, and its potential for functional genomics. *Nucleic Acids Res. 28*, 784–790.
7. Pledger, D. W., Fu, Y. Q., and Coates, C. J. (2004) Analyses of cis-acting elements that affect the transposition of Mos1 mariner transposons in vivo. *Mol. Genet. Genomics 272*, 67–75.
8. Casteret, S., Chbab, N., Cambefort, J., Augé-Gouillou, C., Bigot, Y., and Rouleux-Bonnin, F. (2009) Physical properties of DNA components affecting the transposition efficiency of the mariner Mos1 element. *Mol. Genet. Genomics 282*, 531–542.
9. Leroy, H., Castagnone-Sereno, P., Renault, S., Auge-Gouillou, C., Bigot, Y., and Abad, P. (2003) Characterization of *Mcmar1*, a *mariner*-like element with large inverted terminal repeats (ITRs) from the phytoparasitic nematode *Meloidogyne chitwoodi*. *Gene 304*, 35–41.
10. Augé-Gouillou, C., Hamelin, M. H., Demattéi, M. V., Periquet, G., and Bigot, Y. (2001) The ITR binding domain of the *mariner Mos1* transposase. *Mol. Gen. Genet. 265*, 58–65.
11. Crénès, G., Ivo, D., Hérisson, J., Dion, S., Renault, S., Bigot, Y., and Petit, A. (2009) The bacterial Tn9 chloramphenicol resistance gene: An attractive DNA segment for Mos1 mariner insertions. *Mol. Genet. Genomics 281*, 315–328.
12. Demarre, G., Guerout, A. M., Matsumoto-Mashimo, C., Rowe-Magnus, D. A., Marliere, P., and Mazel, D. (2005) A new family of mobilizable suicide plasmids based on broad host range R388 plasmid (IncW) and RP4 plasmid (IncPα) conjugative machineries and their cognate *Escherichia coli* host strains. *Res. Microbiol. 156*, 245–255.
13. Lipkow, K., Buisine, N., Lampe, D. J., and Chalmers, R. (2004) Early intermediates of mariner transposition: Catalysis without synapsis of the transposon ends suggests a novel architecture of the synaptic complex. *Mol. Cell. Biol. 24*, 8301–8311.
14. Dawson, A., and Finnegan, D. J. (2003) Excision of the *Drosophila mariner* transposon Mos1: Comparison with bacterial transposition and V(D)J recombination. *Mol. Cell 11*, 225–235.
15. Augé-Gouillou, C., Brillet, B., Hamelin, M. H., and Bigot, Y. (2005) Assembly of the mariner Mos1 synaptic complex. *Mol. Cell. Biol. 25*, 2861–2870.
16. Lipkow, K., Buisine, N., and Chalmers, R. (2004) Promiscuous target interactions in the mariner transposon Himar1. *J. Biol. Chem. 279*, 48569–48575.
17. Feschotte, C., Osterlund, M. T., Peeler, R., and Wessler, S. R. (2005) DNA-binding specificity of rice mariner-like transposases and interactions with Stowaway MITEs. *Nucleic Acids Res. 33*, 2153–2165.
18. Cordaux, R., Udit, S., Batzer, M., and Feschotte, C. (2006) Birth of a chimeric primate gene by capture of the transposase gene from a mobile element. *Proc. Natl. Acad. Sci. U.S.A. 21*, 8101–8106.
19. Faure, A., Calmels, C., Desjobert, C., Castroviejo, M., Caumont-Sarcos, A., Tarrago-Litvak, L., Litvak, L. S., and Parissi, V. (2005) HIV-1 integrase crosslinked oligomers are active *in vitro*. *Nucleic Acids Res. 33*, 977–986.
20. Aeling, K. A., Opel, M. L., Steffen, N. R., Tretyanenko, V., Wesley Hatfield, G., Lathrop, R. H., and Senear, D. F. (2006) Indirect recognition in sequence-specific DNA binding by *Escherichia coli* integration host factor. *J. Biol. Chem. 51*, 39236–39248.
21. Thomas, J. O., and Travers, A. A. (2001) HMG1 and 2, and related architectural DNA-binding proteins. *Trends Biochem. Sci. 26*, 167–174.
22. Crellin, P., Sewitz, S., and Chalmers, R. (2004) DNA looping and catalysis: The IHF-folded arm of Tn10 promotes conformational changes and hairpin resolution. *Mol. Cell 13*, 537–547.
23. Canaple, L., Decoville, M., Leng, M., and Locker, D. (1997) The *Drosophila* DSP1 gene encoding an HMG1-like protein: Genomic organization, evolutionary conservation and expression. *Gene 184*, 285–290.
24. Augé-Gouillou, C., Notareschi-Leroy, H., Abad, P., Periquet, G., and Bigot, Y. (2000) Phylogenetic analysis of the functional domains of mariner-like element (MLE) transposases. *Mol. Gen. Genet. 264*, 506–513.
25. Toumi, N. (2006) Caractérisation et analyse fonctionnelle des éléments transposables de type *mariner* issus de deux espèces des sources hydrothemales océaniques (*Bythogreae thermydron* et *Alvinella caudata*). Ph.D. Thesis, University of Le Mans, Le Mans, France.
26. Medhora, M., Maruyama, K., and Hartl, D. L. (1991) Molecular and functional analysis of the mariner mutator element Mos1 in *Drosophila*. *Genetics 128*, 311–318.
27. Lampe, D. J., Churchill, M. E., and Robertson, H. M. (1996) A purified *mariner* transposase is sufficient to mediate transposition in vitro. *EMBO J. 15*, 5470–5479.
28. Liu, D., Bischerour, J., Siddique, A., Buisine, N., Bigot, Y., and Chalmers, R. (2007) The human SETMAR protein preserves most of the activities of the ancestral Hsmar1 transposase. *Mol. Cell. Biol. 27*, 1125–1132.
29. Ivics, Z., Hackett, P. B., Plasterk, R. H., and Izsvák, Z. (1997) Molecular reconstruction of Sleeping Beauty, a Tc1-like transposon from fish, and its transposition in human cells. *Cell 91*, 501–510.
30. Liu, N., Pridgeon, J. W., Wang, H., Liu, Z., and Zhang, L. (2004) Identification of mariner elements from house flies (*Musca domestica*) and German cockroaches (*Blattella germanica*). *Insect Mol. Biol. 13*, 443–447.
31. Delaurière, L., Chénais, B., Pradier, E., Hardivillier, Y., Renault, S., and Casse, N. (2009) DNA binding specificity and cleavage activity of Pacmmar transposase. *Biochemistry 48*, 7279–7286.
32. Miskey, C., Izsvak, Z., Plasterk, R. H., and Ivics, Z. (2003) The *Frog Prince*: A reconstructed transposon from *Rana pipiens* with high transpositionnal activity in vertebrate cells. *Nucleic Acids Res. 31*, 6873–6881.
33. Abad, P., Gouzy, J., Aury, J. M., Castagnone-Sereno, P., Danchin, E. G., Deleury, E., Perfus-Barbeoch, L., Anthouard, V., Artiguenave, F., Blok, V. C., Caillaud, M. C., Coutinho, P. M., Dasilva, C., De Luca, F., Deau, F., Esquibet, M., Flutre, T., Goldstone, J. V., Hamamouch, N., Hewezi, T., Jaillon, O., Jubin, C., Leonetti, P., Magliano, M., Maier, T. R., Markov, G. V., McVeigh, P., Pesole, G., Poulain, J., Robinson-Rechavi, M., Sallet, E., Ségurens, B., Steinbach, D., Tytgat, T., Ugarte, E., van Ghelder, C., Veronico, P., Baum, T. J., Blaxter, M., Bleve-Zacheo, T., Davis, E. L., Ewbank, J. J., Favery, B., Grenier, E., Henrissat, B., Jones, J. T., Laudet, V., Maule, A. G., Quesneville, H., Rosso, M. N., Schiex, T., Smant, G., Weissenbach, J., and Wincker, P. (2009) Genome sequence of the metazoan plant-parasitic nematode *Meloidogyne incognita*. *Nat. Biotechnol. 26*, 909–915.
34. Opperman, C. H., Bird, D. M., Williamson, V. M., Rokhsar, D. S., Burke, M., Cohn, J., Cromer, J., Diener, S., Gajan, J., Graham, S., Houfek, T. D., Liu, Q., Mitros, T., Schaff, J., Schaffer, R., Scholl, E., Sosinski, B. R., Thomas, V. P., and Windham, E. (2008) Sequence and genetic map of *Meloidogyne hapla*: A compact nematode genome for plant parasitism. *Proc. Natl. Acad. Sci. U.S.A. 105*, 14802–14807.
35. Butler, M. G., Chakraborty, S. A., and Lampe, D. J. (2006) The N-terminus of *Himar1 mariner* transposase mediates multiple activities during transposition. *Genetica 127*, 351–366.
36. Richardson, J. M., Colloms, S. D., Finnegan, D. J., and Walkinshaw, M. D. (2009) Molecular architecture of the Mos1 paired-end complex: The structural basis of DNA transposition in a eukaryote. *Cell 138*, 1096–1108.
37. Cui, Z., Geurts, A. M., Liu, G., Kaufman, C. D., and Hackett, P. B. (2002) Structure-function analysis of the inverted terminal repeats of the sleeping beauty transposon. *J. Mol. Biol. 318*, 1221–1235.
38. Izsvák, Z., Khare, D., Behlke, J., Heinemann, U., Plasterk, R. H., and Ivics, Z. (2002) Involvement of a bifunctional, paired-like DNA-binding domain and a transpositional enhancer in Sleeping Beauty transposition. *J. Biol. Chem. 277*, 34581–34588.
39. Moreno-Vázquez, S., Ning, J., and Meyers, B. C. (2005) hATpin, a family of MITE-like hAT mobile elements conserved in diverse plant species that forms highly stable secondary structures. *Plant Mol. Biol. 58*, 869–886.
40. Morgan, G. T. (1995) Identification in the human genome of mobile elements spread by DNA-mediated transposition. *J. Mol. Biol. 25*, 1–5.